Boundary element slope instability modeling of Corinth Canal, Greece due to nearby fault activation

G.-A. Tselentis & F. Gkika
Seismological Laboratory, University of Patras, Greece

Abstract

Corinth Canal is one of the most important civil engineering marine projects in Greece, playing a key role in marine transportation in the Mediterranean. There have been many cases during the past where significant slope instability problems resulted in the abrupt closure of the canal causing serious transportation problems. In this work, three characteristic active faults located in the adjacent area of the Corinth Canal were simulated in order to describe their effect on the canal. Causative deformations and displacements were calculated using boundary element code in 3D grids representing the two sides in the canal. These simulations were conducted in order to define the most dangerous fault which could cause secondary instability effects along the slopes of the canal and to assess the damage distribution along the axis of the canal pinpointing regions of high instability risk.
Keywords: slope instability, rupture propagation, Corinth Canal, Greece.

1   Introduction

Corinth Canal is one of the most important civil engineering marine projects that were constructed in Greece during the 19th century, Figure 1. Geographically is located in the eastern border of the Corinth Gulf which is an asymmetric half-graben one of the most rapid developed intercontinental rifts in Europe. High seismicity concentration in the gulf shows that tectonic activity still takes place in this area, (e.g. Tselentis and Macropoulos [21], Billiris et al [2], Clarke et al [3], Doutsos and Kokkalas [8]).

Since the opening of the canal in 1893 several problems due to local slope instabilities have been reported. Most of them occur in the Peloponnesus side. During the 2nd half of the 20th century 16 local slope instabilities have occurred in this area.
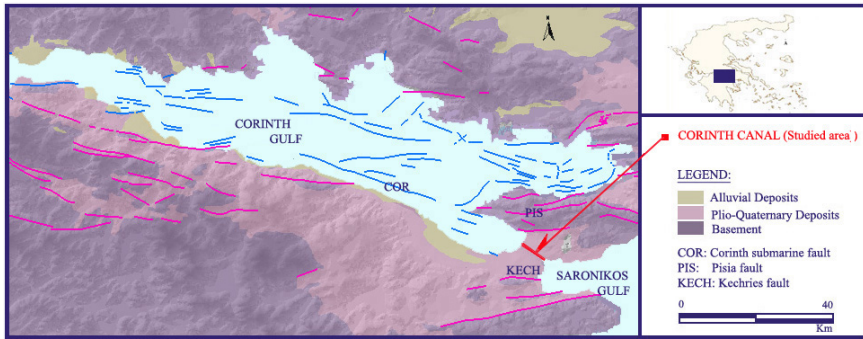

Figure 1:   Studied area, with the three simulated faults Corinth, Pisia and Kechries.

Corinth Canal is 6.3 km long, striking NW-SE. The canal seems to be formed by antitilted fault blocks that create a series of tectonic grabens and horsts. The northern system of the block-faulted area has its greatest height in the East and dips below the sea level towards the west, while the system in the south acts reversely. A neutral zone exists between them tilted to a lesser degree, (Freyberg [9]).

The main formations that can be seen in the Canal region are Neogene and Quaternary sediments. These are alternating layers of silty marl, marly sandstone, conglomerates and marly limestone intercalated at places by layers of marly clays, silts, sands and gravel, (Andrikopoulou et al [1]). In Figure 2, it can be seen that the marly formation dominates in the central horst block of the Corinth Canal furthermore there exists an upwards sub-sequence transition from fresh or brackish water facies (grey to bluish grey marls) to marine sediments (light yellow marls and the series of Pleisto-Holocene beach to shoreface subsequences), (Collier [4]).

The Neogene and Quaternary sediments in the canal are cut by numerous sub-vertical faults with nearly East-West striking. During the latest geotechnical zoning 52 main faults were mapped by Andrikopoulou et al [1]. These faults are crossed by a major system of subvertical joints running parallel to them at an angle 30° to 40° degrees with respect to the Canal axis, (Cristoulas et al [6]).

In the past century three earthquakes 1928, 1953 and 1981 with epicenters located in the adjacent area of the canal have been associated with moderate to minor surface faulting. During the earthquakes of 1928 and 1981, two different known fault reactivations and localized instabilities have been reported in the canal.
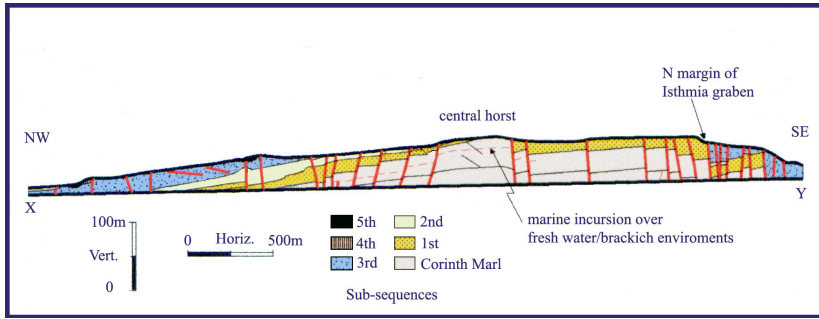
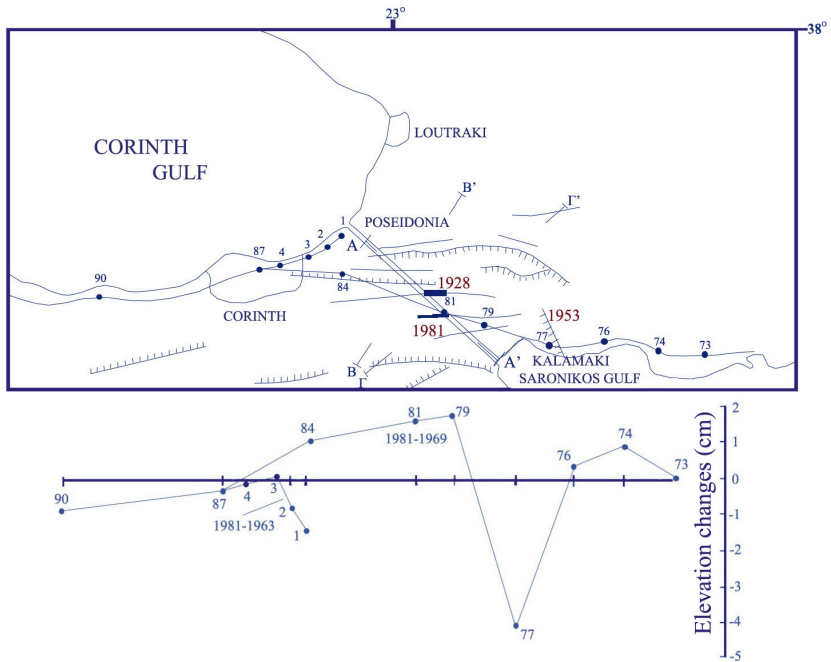Figure 2:   Geological section of Corinth Canal.

Figure 3:   Main faults, seismic faulting (thick lines) and leveling benchmarks of
the geodetic surveys. Elevation changes along leveling routes based
on geodetic measurements are depicted, Mariolakos and Stiros [16].

The last event was probably associated with small but significant motions
detected by geodetic data, (Mariolakos and Stiros [16]), Figure 3.

The displacement profile presented in this geodetic investigation revealed that
the central part of Corinth Canal appears uplifted relative to the near-coastal
areas whereas Possidonia shows a trend of subsidence relative to Corinth. The
authors believe that the deformation trend in the Corinth Canal has not

significantly changed since the Quaternary and the mechanism of deformation of the canal area is similar to platelike body under torsion. On the contrary Collier [4] has found no genetically compressive structures to support this hypothesis of Mariolakos and Stiros [16]. The authors believe that the uplift of the Corinth Canal is one of two tectonic displacement vectors affecting the area and the other is extensional fault induced subsidence, which latter may be accompanied by block rotations.

2 Numerical modelling

We use numerical models to examine the stress field around idealized normal faults in order to investigate instability regions along the canal. The 3-D numerical method addresses the effects of fault tipline shape and mechanical interaction of fault segments upon the numerical solution to the perturbed stress field. Using the underlying assumption that joints are opening mode cracks that form perpendicular to least compressive principal stresses of sufficient magnitude to break the canals slope material, we determine locations that might possess a high degree of instability as a consequence of fault slip.

2.1 Modeling method

We computed solutions to boundary value models of normal faults imbedded in an elastic half-space using the program Poly3D, (Thomas, [20]). Based upon the boundary element method (Crouch and Starfield [7]), Poly3D incorporates the fundamental solution to an angular dislocation in a homogeneous, linear elastic half-space (Comninou and Dundurs [5]; Jeyakumaran et al [13]). A number of angular dislocations are juxtaposed to create polygonal boundary elements that collectively define discretized objects of arbitrary shape in three dimensions. The basic principle of Poly3D is depicted in Figure 4A.

Boundary conditions in Poly3D can be applied remotely (as constant stresses or strains), at the centers of each element of the discretized crack surface (as tractions or displacements), or as combinations thereof. The program solves a series of linear algebraic equations that describe the influence on each element of every other element under a prescribed set of boundary conditions. Once the displacement distribution along a fault is determined, the static stress, strain and displacement fields around the fault are calculated using influence coefficient equations that relate the displacements at the fault to the resultant elastic field at any point in the surrounding linear elastic medium. This solution is superimposed upon the remote stress field boundary condition to produce the total elastic field. The governing equations implemented by Poly3D are described in Thomas [20].

An example of a POLY3D implementation is presented in Figure 4B. Overlapping fault elements are prescribed with the condition of zero opening or interpenetration.
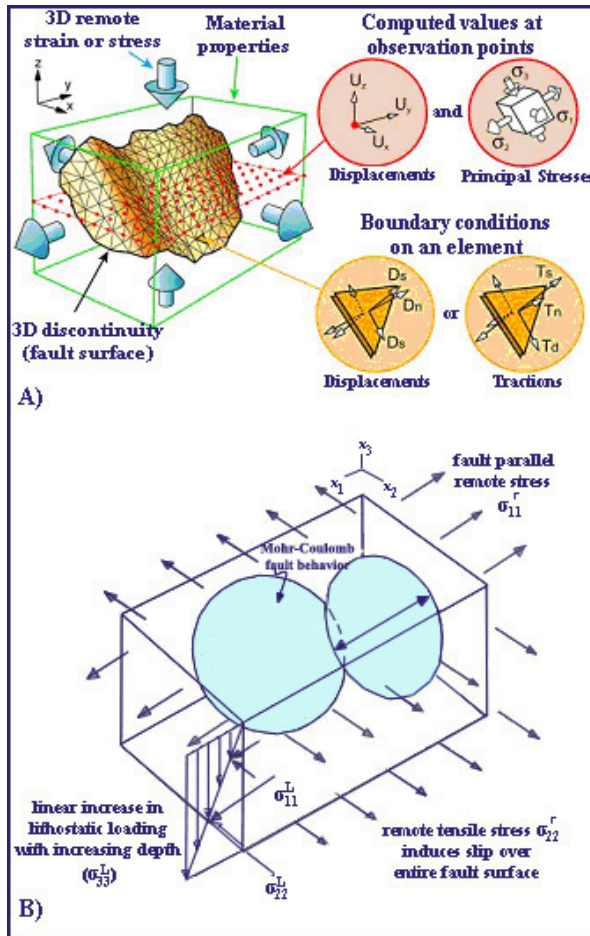
Figure 4: A) Model configuration for fault in an infinite elastic body, Thomas [20] B) Overlapping Faults modelling in POLY3D.Boundary conditions include a remote tectonic tension driving fault slip (sr22), a fault-parallel remote tectonic stress (sr11), and an increasing lithostatic load with increasing depth (sLij). The combined remote and lithostatic stresses produce a state of all-round compression in the vicinity of the fault, Kattenhorn et al [15].

Frictional resistance to slip on the fault, the implementation of which is described by Kattenhorn [14], accounts for the effect of an increasing lithostatic load along the fault surface in the down-dip direction. Fault slip is governed by a simple Coulomb frictional slip criterion, and is driven by a constant, remote

tectonic tension applied perpendicular to fault strike, sufficient to promote slip over the entire fault surface.

2.2 Simulation results

Three characteristic active faults located in the adjacent area of the Corinth Canal were simulated in order to describe the potential hazard due to secondary earthquake effects on the slopes of the canal. These active sources were the Corinth offshore fault and the onshore faults Pisia and Kechries, Figure 1.

   Corinth fault was selected due its high seismic risk contribution in the canal area (Gkika et al [10]), it has a length of about 26km and is the longest fault on the southern margin of the Corinth Gulf. It trends WNW-ESE almost parallel to the coastline and dips at approximately 35-46° to the north, producing a scarp of 650m height. Corinth fault exhibits the characteristics of a continuously active fault. This observation is confirmed by the thickening of the upper sediment strata towards the fault plane and the observation that the onshore rivers Sithas, Agiorgitikos and Fonissa dip more steeply in their equivalent offshore canyons indicating high slip rate. In addition, this is further supported by the raised marine terraces in the coastal zone and provides evidence of coseismic activity, (Stefatos et al [19]).

   Pisia onshore fault had been reactivated (up to 1m vertical downthrown) during the Alkionides earthquakes main aftershock on 25-2-1981 with magnitude 6.4 R. It is a normal fault dipping to the north, with an E-W direction and a total length up to 15km, Jackson et al [12]. Finally, Kechries fault is evident that has been closely related with two episodes of submergence at the ancient Kechreai port during the AD 400 and AD 1928 earthquakes, (Noller et al [18]).

   All off the above mentioned faults are located close to the Canal and they were chosen because of their potential damage in case of activation. Table 1 describes the rupture inputs that where used in order to simulate fault activation.

Table 1: Description of the rupture inputs that where used in our models in order to simulate Corinth, Pisia and Kechries fault reactivation.

ID	FAULT NAME	LENGTH (Km)	DEPTH (Km)	dip (^{o})	DISPLACEMENT (m)
1	CORINTH	13	5	45	1
2	PISIA	7.5	5	45	1
3	KECHRIES	4	4	50	0.5

   The model material was described by the elastic constants of Young's modulus E= 70.000 MPa and Poisson's ratio v = 0.25, which where chosen as most representative for the region of the eastern Corinth Gulf, Hubert et al [11].
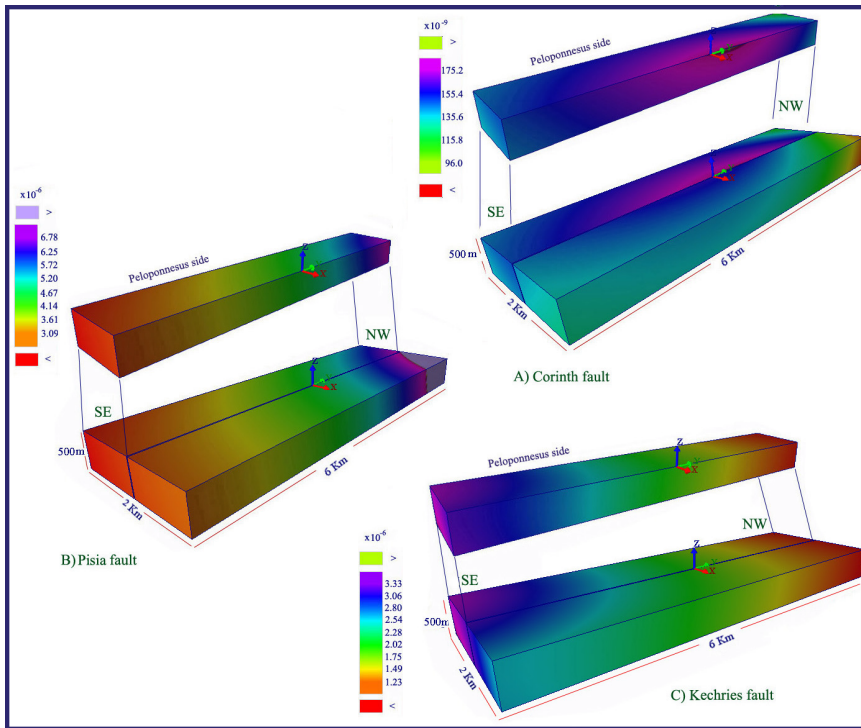
Figure 5:   Deformation distribution simulated along the axis of the Corinth Canal due to the activation of A) Corinth, B) Pisia and C) Kechries faults. The center of the canal is indicated with the arrows.

By simulating the activation of these faults, causative deformations and displacements were calculated in two 3D grids which were representing the two sides of the Corinth Canal (Peloponnesus and Continental Greece side). Figure 5 and 6 depict the calculated deformations and displacements in the vicinity of Corinth Canal respectively.

The displacement and deformation distributions are calculated in two 3D grids having a distance of 20m between them. Each grid has dimensions of 6km (length) x 1km (wide) x 0.5km (depth) and with a step of 50m x 20m x 10m along each axis respectively.

3   Conclusions

The calculated deformations along the Corinth Canal due to the simulated activation of the three studied faults are relative small, in the order of 10^{-6}. Although the Corinth fault is the largest of the three its activation result in smaller deformations along the Canal as compared with the effects of Pisia and

Kechries faults. In the hypothetical case of Pisia fault activation we can notice that the deformations distribution is towards the NE part of the Canal on the Continental Greece side, Figure 5. The maximum displacements along the axis of the canal (U_y) are expected to range approximately between 2.2 and 5cm, Figure 6. Changes of the deformations and displacements distribution are focused mainly in the central part of the Canal between sites 3.000-4.000m. In this area instability effects are expected to be more serious. Finally as far as Kechries fault is considered, smaller deformations are expected towards the SW section of the Canal and between the sites 3900-5000m.
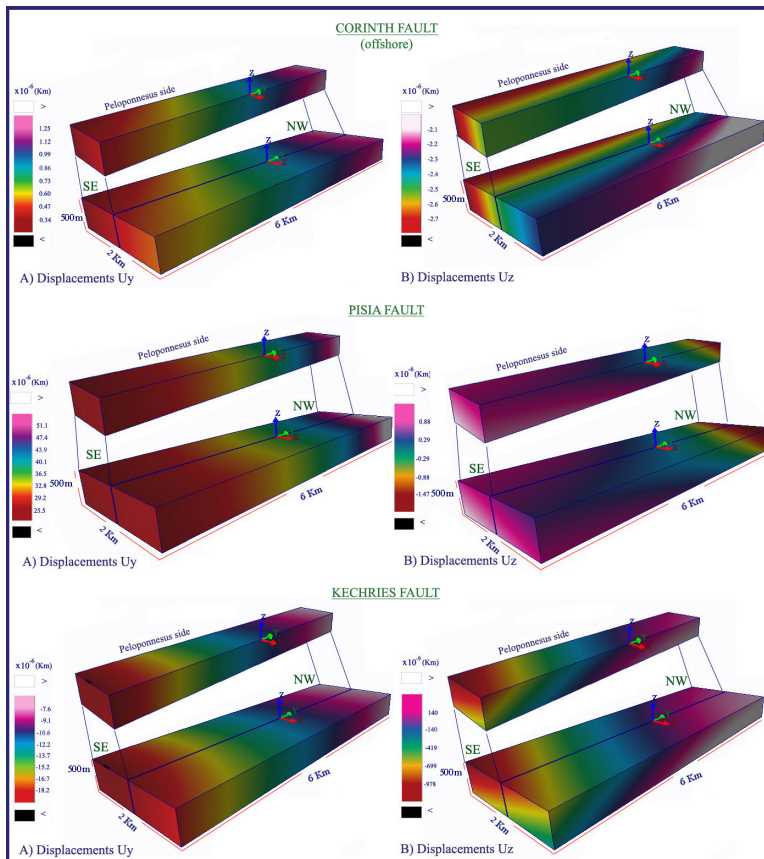

Figure 6: Displacement distribution in the Corinth Canal A) along the axis of the canal Uy and B) the depth Uz, due to the activation of Corinth, Pisia and Kechries fault. The center of the canal is indicated with the arrows.

Acknowledgements

References

[1]   Andrikopoulou K. P., Marinos P. G., Vainalis D., Geotechnical zoning in the Corinth Canal, Engineering Geology of Ancient Works, Monuments and Historical Sites, Athens, Greece, Balkema, 1, pp. 231-235, 1988.Becker A.A., The Boundary Element Method in Engineering, McGraw-Hill, New York, 1992.

[2]   Billiris H., Paradissis D., Veis G., England P., Featherstone W., Parsons B., Cross P., Rands P., Rayson M., Sellers P., Ashkenazi V., Davison M., Jackson J., Ambraseys N. N., Geodetic determination of tectonic deformation in central Greece from 1900 to 1988, Nature, 350, pp. 124-129, 1991.

[3]   Clarke P. J., Davies R. R., England P. C., Parsons B. E., Billiris H., Paradissis D., Veis G., Denys P. H., Cross P. A., Ashkenazi V., Bingley R., Geodetic estimate of seismic hazard in the Gulf of Korinthos, Geophys. Res. Lett., 24, pp. 1303-1306, 1997.

[4]   Collier R. E., Eustatic and tectonic controls upon Quaternary coastal sedimentation in the Corinth Basin, Greece, Journal of the Geological Society, London, 147, pp.301-316, 1990.

[5]   Comninou M.A. and Dunders J., The angular dislocation in a half-space, Journal of Elasticity, 5, pp. 203-216, 1975.

[6]   Cristoulas S.G., Kalteziotis N.A., Tsiabaos G.K., Geotechnical problems in a bridge over Corinth Canal, Int. Conf. on Case Histories in Geotechnical Engineering, St Louis, Missouri, 3, pp. 849-54, 1984.

[7]   Crouch S.L. and Starfield A.M., Boundary Element Methods in Solid Mechanics, Unwin Hyman, London, 1983.

[8]   Doutsos T., Kokkalas S., Stress and deformation patterns in the Aegian region, Journal of Structural Geology, 23, pp. 455-472, 2001.

[9]   Freyberg V., Geologie des Isthmus von Korinth, Erlangen Geologische Ablhandlungen, 95, pp. 1-183., 1973.

[10]   Gkika F., Tselentis G-A., Danciu L., Seismic risk assessment of Corinth Canal Greece, in this volume.

[11]   Hubert A., King J., Armijo R., Bertrand M., Papanastasiou D., Fault re-activation, stress interaction and rupture propagation on the 1981 Corinth earthquake sequence, Earth and Planetary Science Letters, 42, pp. 573-585, 1996.

[12]   Jackson J. A., Gagnepain J., Houseman G., King G. C. P., Papadimitriou P., Soufleris C., Virieux J, Seismicity, normal faulting and the geomorphological development of the Gulf of Corinth (Greece), the

Corinth earthquakes of February and March 1981, Earth. Planet. Science Letters, 57, pp. 377-397, 1982.

[13] Jeyakumaran M., Rudnicki J.W., Keer L.M., Modeling slip zones with triangular dislocation elements, Bulletin of the Seismological Society of America, 82, pp. 2153-2169, 1992.

[14] Kattenhorn S.A., A 3D mechanical analysis of normal fault evolution and joint development in perturbed stress fields around normal faults, Unpublished Ph.D. thesis, Stanford University, Stanford, California, U.S.A., 1998.

[15] Kattenhorn S.A., Audin A., Pollard D.D., Joints and high angles to normal fault strike: an explanation using 3D numerical models of fault-perturbed stress fields, Journal of Structural Geology, 22, pp. 1-23, 2000.

[16] Mariolakos I., Stiros S. C., Quaternary deformation of the Isthmus and Gulf of Corinthos (Greece), Geology, 15, pp. 225–228, 1987.

[17] McGarr A., On the state of lithospheric stress in the absence of applied tectonic forces, Journal of Geophysical Research, 93, pp.13609-13617, 1988.

[18] Noller J.S., Wells L.E., Reinhardt E., Rothaus R.M., Subsidence of the Harbour at Kenchreai, Saronic Gulf, Greece, During the earthquakes of AD 400 and AD 1928, American Geophysical Union Transactions, 78, pp. 636, 1997.

[19] Stefatos A., Papatheodorou G., Ferentinos G., Leeder M., Collier R., Seismic reflection imaging of active offshore faults in the Gulf of Corinth: their seismotectonic significance, Basin Research, 14, pp. 487-502, 2002.

[20] Thomas A.L., Poly3D: A three-dimensional, polygonal element, displacement discontinuity boundary element computer program with applications to fractures, faults, and cavities in the Earth's crust. MS thesis, Stanford University, 1993.

[21] Tselentis G-A., Makropoulos K., Rates of crustal deformation in the gulf of Corinth (central Greece) as determined from seismicity, Tectonophysics, 124, pp.55-66, 1986.